

Dynamics of the fcc Heisenberg antiferromagnet with nearest-neighbor interactions. II. Dilute arrays

W. Y. Ching

Department of Physics, University of Missouri—Kansas City, Kansas City, Missouri 64110

D. L. Huber

Department of Physics, University of Wisconsin, Madison, Wisconsin 53706

(Received 27 May 1982)

We report the results of a study of the dynamics of the site-dilute face-centered-cubic Heisenberg antiferromagnet with nearest-neighbor interactions. Numerical techniques are used to obtain information about the effect of dilution on the distributions of local fields in the various equilibrium spin configurations. Spin excitations are studied within the framework of a linearized magnon theory. The density of magnon modes is determined for 50% dilution and compared with the corresponding results for the fully occupied lattice and an antiferromagnet with type-III long-range order. The equations of motion for the spins are integrated to obtain the dynamic structure factor. The peaks in the dynamic structure factor indicate the existence of damped spin waves which mirror the short-range-order characteristic of the fully occupied lattice. We find no evidence for weakly damped, long-wavelength hydrodynamic spin waves. The relation of the work to experimental studies of the dilute semiconductors $\text{Cd}_{1-c}\text{Mn}_c\text{Te}$, $\text{Hg}_{1-c}\text{Mn}_c\text{Te}$, and $\text{Zn}_{1-c}\text{Mn}_c\text{Te}$ is commented on.

I. INTRODUCTION

In a recent paper¹ (hereafter referred to as I) we have reported the results of a study of the ground-state spin configurations and the harmonic collective excitations of a face-centered-cubic Heisenberg antiferromagnet with nearest-neighbor interactions. The calculations were carried out on a fully occupied lattice. In this paper we extend the analysis begun in I to dilute arrays where a fraction $1-c$ of the spins are removed at random. We report results for the distribution of local fields, the density of states, and the positions and widths of the peaks in the dynamic structure factor. The emphasis in this paper is on the effect of dilution of the spin dynamics of the fcc system with *nearest-neighbor* interactions. The calculations reported here may contribute to the understanding of the low-temperature properties of the dilute magnetic semiconductors $\text{Cd}_{1-c}\text{Mn}_c\text{Te}$, $\text{Hg}_{1-c}\text{Mn}_c\text{Te}$, and $\text{Zn}_{1-c}\text{Mn}_c\text{Te}$, where the Mn ions are located on an fcc lattice.²⁻⁶ However, quantitative comparisons between numerical calculations and various experimental results require more detailed information about the exchange interactions (nearest *and* next-nearest neighbor) than is currently available.

In the remainder of this section we summarize the results of I that are relevant to the behavior of dilute arrays. In Sec. II we consider the effect of dilution on the local fields. Spin dynamics is considered in Sec. III, while in Sec. IV we discuss our results with emphasis on the question of the existence of hydrodynamic spin-wave modes in spin-glasses. We also comment on the relation of our results to recent measurements of the Raman spectrum of $\text{Cd}_{1-c}\text{Mn}_c\text{Te}$.⁴

As noted in I the fcc Heisenberg antiferromagnet with nearest-neighbor interactions is an example of a frustrated system with a highly degenerate ground state. Although there is no three-dimensional long-range order, each spin experiences the same local exchange field $-4J$, while the magnetization is identically equal to zero.⁷ In I two classes of classical ground-state spin configurations were identified. In class-I states spins in (001) planes were antiferromagnetically coupled (i.e., two-dimensional long-range order), with the direction of the antiferromagnetic axis randomly from plane to plane. The second class of configurations, which are probably less numerous, can be regarded as defective class-I states.

Calculations of the dynamic structure factor indi-

cated that the harmonic magnons for both class-I and class-II ground states resembled those of an antiferromagnet with type-III three-dimensional

long-range order. In type-III antiferromagnets with nearest-neighbor interactions the spin-wave energy takes the form ($\hbar=1$)

$$\omega(\vec{q}) = 4J \left[\cos(q_x/2)\cos(q_y/2) + \cos(q_x/2)\cos(q_z/2) + \cos(q_y/2)\cos(q_z/2) + 1 \right]^{1/2} \left[1 - \cos(q_x/2)\cos(q_y/2) \right]^{1/2} \tag{1}$$

for unit spin ($S=1$) and lattice constant. Here J denotes the exchange integral in the Heisenberg interaction

$$\mathcal{H} = \sum'_{(i,j)} J \vec{S}_i \cdot \vec{S}_j, \tag{2}$$

where the prime signifies that the sum is restricted to nearest-neighbor pairs. There was nearly complete agreement between the numerical results and Eq. (1) for \vec{q} along [110], [111], and [001] (where the modes had zero frequency); with \vec{q} along [100] the modes for the disordered system were somewhat higher in energy than the spin waves in a type-III antiferromagnet. In all cases the peaks in the dynamic structure factor were "resolution limited," having a width determined by the exponential cut-off in the numerical integration.

II. GROUND-STATE PROPERTIES

As noted above, despite the absence of three-dimensional long-range order, the spins in the fully occupied lattice show a high degree of correlation as evidenced by the fact that each spin experiences the same local field $-4J$. Diluting the array produces a shift and broadening of the distribution of local fields. This is shown in Fig. 1 where the histograms of the local-field values are displayed for an array of 2048 sites with periodic boundary conditions. These results were obtained by minimizing the energy of the classical Hamiltonian (2) using methods discussed elsewhere.^{1,8,9}

Particularly noticeable is the breadth of the distribution for $c=0.9$. It is evident that a relatively small amount of compositional disorder has a pronounced effect on the spin correlations. Below $c=0.4$ the histograms begin to show spikes reflecting the contributions from isolated spins, pairs, triples, etc.

From this figure it is apparent that there is also a shift in the mean value of the local field, which is twice the average energy per spin $\langle E \rangle / J$. Results for $\langle E \rangle / J$ for various values of c are given in Ref. 7. For $c > 0.5$ we have the approximate relation

$$\langle E \rangle / J \simeq -2 + (1 - c), \tag{3}$$

suggesting that the contributions to $\langle E \rangle / J$ from terms of order $(1 - c)^2$ are small.

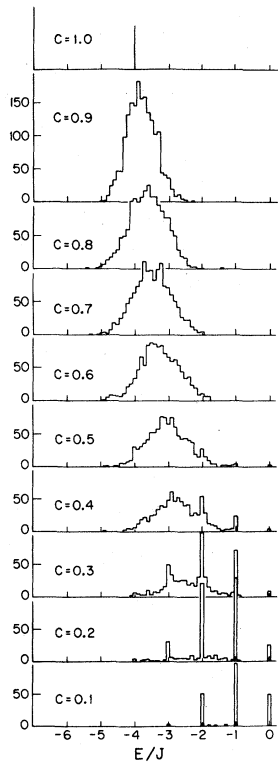


FIG. 1. Distribution of local fields for array of 2048 sites; c denotes the fraction of occupied sites. When $c=1$ all local fields are equal to $-4J$.

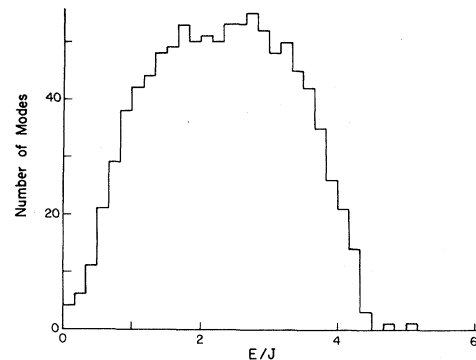


FIG. 2. Distribution of magnon modes for $c=0.5$. The array has 500 sites of which half are occupied at random. The histogram displays the data from four configurations.

Recently Grest and Gabl¹⁰ have studied the thermodynamic properties of the dilute fcc *Ising* antiferromagnet with nearest-neighbor interactions using Monte Carlo techniques. They find that the system freezes into a spin-glass phase for $0.18 \leq c \leq 0.40 \pm 0.10$. The data in Fig. 1 show no evidence of an abrupt change of character in the ground state in this concentration range. Rather, we find the only qualitative change in the local-field distribution occurring between $c=0.9$ and 1.0.

III. SPIN DYNAMICS

The analysis of the spin dynamics follows the pattern of an earlier work on the dynamics of the Edwards-Anderson model^{8,9} in that we calculate the magnon energies and the dynamic structure factor from the linearized equations of motion for the spins. Our results for the distribution of magnon modes for $c=0.5$ are shown in Fig. 2 where we display the data obtained from a total of four configurations each with 250 spins (500 sites with 50% occupancy).

Figure 2 is to be compared with the corresponding results for the fully occupied lattice and the

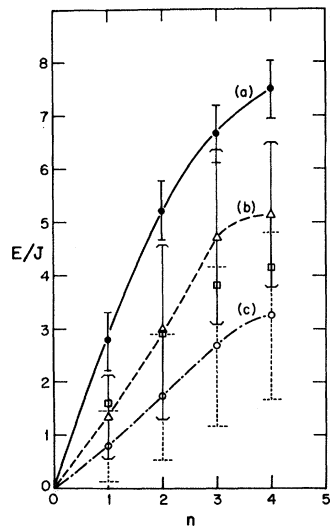


FIG. 3. Location and width of the peaks in the dynamic structure factor for $\vec{q}=(\pi/4)(n,0,0)$. The results for $c=1.0$ are shown as solid circles, for $c=0.9$ as open triangles, for $c=0.5$ as open circles. The open squares are from Eq. (5) with $c=0.9$. The error bars denote the width of the peaks at half-height. The solid bars refer to the result for $c=1.0$; the bracketed bars to $c=0.9$, and the broken-line bars to $c=0.5$. Results from single configurations of arrays with $2048c$ spins.

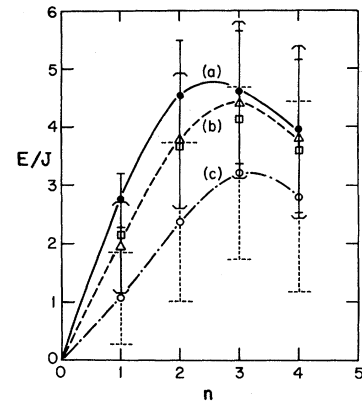


FIG. 4. Same as Fig. 3 except $\vec{q}=(\pi/4)(n,n,0)$.

type-III antiferromagnet which were given in I. It is apparent that dilution has the effect of reducing the number of high-frequency modes ($E > 4J$) while at the same time smoothing out the fine structure associated with the critical points in the Brillouin zone. Also evident is the absence of "zero frequency" modes. As noted in the Introduction, modes with \vec{q} along [001] have a vanishing frequency in both the type-III and the fully occupied random antiferromagnet. In the dilute system the excitations are isotropic at long wavelengths since the [100], [010], and [001] directions are equivalent. In contrast to the Edwards-Anderson model^{8,9} and $\text{Eu}_x\text{Sr}_{1-x}\text{S}$ ($x=0.40$ and 0.54)¹¹ the density of states decreases rapidly as $E \rightarrow 0$. However, a finite density at the origin cannot be ruled out.

As shown in Ref. 9 we can obtain an expression for the zero-temperature dynamic structure factor $S(\vec{q}, E)$ by integrating the equations of motion for the spins, i.e.,

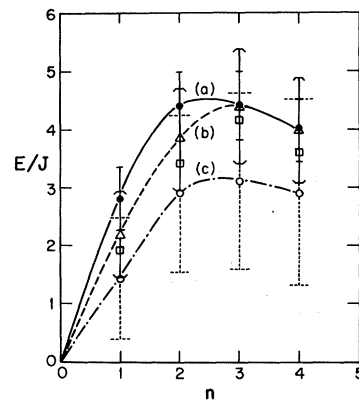


FIG. 5. Same as Fig. 3 except $\vec{q}=(\pi/4)(n,n,n)$.

$$S(\vec{q}, E) = (i/\pi) \sum_{\alpha=x,y,z} \int_0^{\infty} \sin(Et) \langle [S_{\alpha}(\vec{q}, t), S_{\alpha}(-\vec{q}, 0)] \rangle dt. \quad (4)$$

We have calculated $S(\vec{q}, E)$ for \vec{q} along [100], [110], and [111] for $c=0.9$ and 0.5. In all cases we obtained a dominant peak whose width and location shifted with \vec{q} . In Figs. 3–5 we display the location and halfwidths of the two dilute systems along with our results for $c=1.0$. The data were obtained with an exponential cut-off in the integrand (4) which gave rise to an “instrumental” width of $0.5J$. All data are from single configurations associated with an array of 2048 sites.

Also shown in Figs. 3–5 are points for $c=0.9$ which are calculated from an approximate dispersion curve derived by multiplying the square root of the cubic average of the square of the spin-wave frequency of a type-III antiferromagnet [Eq. (1)] by the fractional occupancy, i.e.,

$$\omega(\vec{q})_{\text{approx}} = 4cJ [\cos(q_x/2)\cos(q_y/2) + \cos(q_x/2)\cos(q_z/2) + \cos(q_y/2)\cos(q_z/2) + 1]^{1/2} \\ \times \left\{ 1 - \frac{1}{3} [\cos(q_x/2)\cos(q_y/2) + \cos(q_x/2)\cos(q_z/2) + \cos(q_y/2)\cos(q_z/2)] \right\}^{1/2}. \quad (5)$$

Apart from the high-frequency modes with \vec{q} along the [100] directions the agreement between (5) and our numerical results for $c=0.9$ is quite reasonable. (The discrepancy observed with \vec{q} along [100] is analogous to what we found in our study of the fully occupied lattice.¹) We interpret this agreement as indicating that the peaks in the dynamic structure factor mirror a short-range-order characteristic of the fully occupied lattice.

IV. DISCUSSION

The data shown in Figs. 3–5 appear to indicate the existence of damped spin-wave modes in the dilute fcc antiferromagnet. However, care should be exercised in interpreting the numerical results for $S(\vec{q}, E)$ since an exponential cutoff $\exp[-\Gamma t]$ in the integrand for the structure factor [Eq. (4)] will generate a peak even when $\langle [S_{\alpha}(\vec{q}, t), S_{\alpha}(-\vec{q}, 0)] \rangle$ is independent of time. Additional insight into the

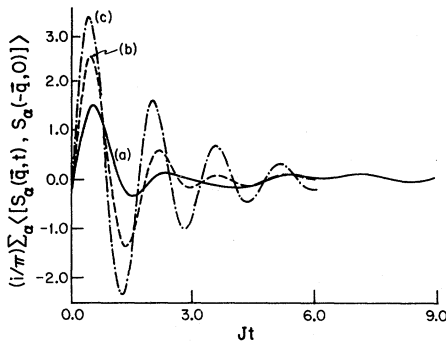


FIG. 6. $(i/\pi) \sum_{\alpha} \langle [S_{\alpha}(\vec{q}, t), S_{\alpha}(-\vec{q}, 0)] \rangle$ vs Jt for $c=0.9$. Single configuration of an array with 2048 sites. (a) $\vec{q}=(\pi/2)(1,0,0)$; (b) $\vec{q}=(\pi/2)(1,1,0)$; (c) $\vec{q}=(\pi/2)(1,1,1)$. The function plotted is proportional to the sine transform of $S(q, E)$.

dynamics can be gained from a direct analysis of the integrand (without the sine factor). In Figs. 6–8 we show our results for $(i/\pi) \langle [S_{\alpha}(\vec{q}, t), S_{\alpha}(-\vec{q}, 0)] \rangle$ for various values of c and \vec{q} .

Figure 6 displays the results for $c=0.9$, $\vec{q}=(\pi/2)(1,0,0)$, $(\pi/2)(1,1,0)$, and $(\pi/2)(1,1,1)$, while the data for the same q values are displayed in Fig. 7 for $c=0.5$. A comparison of the two figures shows that the effect of dilution is to enhance the damping for modes of equivalent wave vector.

An interesting question concerns the existence of so-called hydrodynamic spin-wave modes which are weakly damped, low-frequency propagating excitations with an energy proportional to q and a width proportional to q^2 .¹² As in the case of the Edwards-Anderson model¹³ we find no evidence for such modes. Instead, it appears that the modes become more heavily damped with decreasing \vec{q} . In Fig. 8 we show our results for $q=(\pi/4)(1,0,0)$, $c=0.6, 0.9$, and for $\vec{q}=\pi(1,0,0)$, $c=0.6$. From this figure it is evident that for a given concentration ($c < 1$) the long-wavelength excitations are

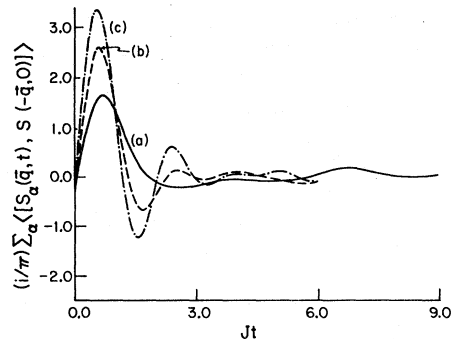


FIG. 7. Same as Fig. 6 except $c=0.5$. (a) $\vec{q}=(\pi/2)(1,0,0)$; (b) $\vec{q}=(\pi/2)(1,1,0)$; (c) $\vec{q}=(\pi/2) \times (1,1,1)$.

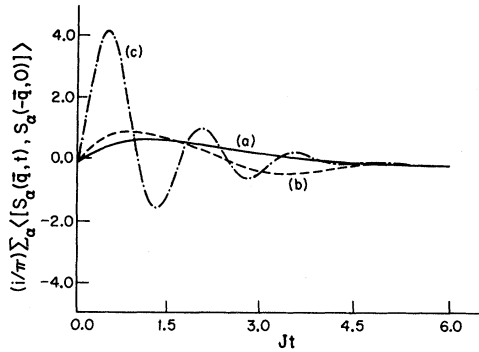


FIG. 8. Same as Fig. 6 except (a) $c=0.6$, $\vec{q}=(\pi/4)(1,0,0)$; (b) $c=0.9$, $\vec{q}=(\pi/4)(1,0,0)$; (c) $c=0.6$, $\vec{q}=\pi(1,0,0)$.

more heavily damped than those of shorter wavelength. This result is consistent with our earlier comments about the excitations mirroring the short-range order associated with the high- q Fourier components.

Finally, we would like to comment further on the connection between our results obtained for an fcc lattice with nearest-neighbor (NN) interactions and the behavior of the dilute magnetic semiconductors $\text{Cd}_{1-c}\text{Mn}_c\text{Te}$, $\text{Hg}_{1-c}\text{Mn}_c\text{Te}$, and $\text{Zn}_{1-c}\text{Mn}_c\text{Te}$. The most thoroughly studied material in this class, $\text{Cd}_{1-c}\text{Mn}_c\text{Te}$, shows spin-glass behavior for $0.17 \leq c \leq 0.60$ and type-III antiferromagnetic order for $0.60 \leq c \leq 0.71$.^{2,3} Above $c=0.71$ the material undergoes a transition to the zincite structure. Were this transition not to take place it is likely

that the type-III order persist to $c=1.0$. On the basis of molecular-field and spin-wave analyses it can be shown that stable type-III order in a fully occupied lattice requires a next-nearest-neighbor (NNN) interaction in the range $0 < J_{\text{NNN}} < 0.5J_{\text{NN}}$.¹⁴⁻¹⁶ Because of the presence of the next-nearest-neighbor interactions our results cannot be compared directly with experiment.¹⁷ However, we note that a one-magnon peak was observed in the Raman spectrum of the spin-glass phase of $\text{Cd}_{1-c}\text{Mn}_c\text{Te}$.⁴ Identifying the position of the peak, $4.5-5.5 \text{ cm}^{-1}$ for $c=0.4-0.5$, with the maximum in the density of states for $c=0.5$ (Fig. 2), $E_{\text{max}} \approx 2.2J$, we infer an effective nearest-neighbor exchange interaction $\sim 0.8-1.0 \text{ cm}^{-1}$ in reasonable agreement with the estimate $0.76 \pm 0.07 \text{ cm}^{-1}$ obtained from an analysis of the specific heat and susceptibility of exchange-coupled pairs.^{2,18}

Note added in proof. Recent neutron scattering studies of $\text{Cd}_{1-c}\text{Mn}_c\text{Te}$ [T. Giebultowicz, W. Minor, B. Buras, B. Lebech, and R. R. Galazka, Phys. Scr. **25**, 751 (1982)] indicate the absence of true long-range order in the type-III regime $0.60 \leq c \leq 0.71$.

ACKNOWLEDGMENT

This research was supported in part by the National Science Foundation (NSF) under Grant No. DMR-7904154 and by the University of Missouri-Kansas City Research Council.

- ¹W. Y. Ching and D. L. Huber, Phys. Rev. B **25**, 5761 (1982).
- ²R. R. Galazka, S. Nagata, and P. H. Keesom, Phys. Rev. B **22**, 3344 (1980).
- ³T. Giebultowicz, H. Kepa, B. Buras, K. Clausen, and R. R. Galazka, Solid State Commun. **40**, 499 (1981).
- ⁴S. Venugopalan, A. Petrou, R. R. Galazka, A. K. Ramdas, and S. Rodriguez, Phys. Rev. B **25**, 2681 (1982).
- ⁵S. Nagata, R. R. Galazka, D. P. Mullin, H. Akbarzadeh, G. D. Khattak, J. K. Furdyna, and P. H. Keesom, Phys. Rev. B **22**, 3331 (1980).
- ⁶T. M. Holden, G. Dolling, V. F. Sears, J. K. Furdyna, and W. Giriat, Solid State Commun. **40**, 281 (1981).
- ⁷W. Y. Ching and D. L. Huber, J. Appl. Phys. **52**, 1715 (1981).
- ⁸W. Y. Ching, K. M. Leung, and D. L. Huber, Phys. Rev. Lett. **39**, 729 (1977).
- ⁹W. Y. Ching, K. M. Leung, and D. L. Huber, Phys. Rev. B **23**, 6126 (1981).
- ¹⁰G. S. Grest and E. G. Gahl, Phys. Rev. Lett. **43**, 1182

(1979).

- ¹¹W. Y. Ching, K. M. Leung, and D. L. Huber, Phys. Rev. B **21**, 3708 (1980).
- ¹²B. I. Halperin and W. M. Saslow, Phys. Rev. B **16**, 2154 (1977).
- ¹³See Ref. 9. We have obtained similar results for $\text{Eu}_x\text{Sr}_{1-x}\text{S}$ ($x=0.40$ and 0.54). In this case the short-wavelength excitations mirror the short-range ferromagnetic order of EuS . The long-wavelength modes appear to be overdamped in the spin-glass phase.
- ¹⁴J. S. Smart, *Effective Field Theories of Magnetism* (Saunders, New York, 1966), p. 77.
- ¹⁵D. ter Haar and M. E. Lines, Philos. Trans. R. Soc. London, Ser. A **254**, 521 (1962); **255**, 1 (1962).
- ¹⁶M. E. Lines, Proc. R. Soc. London, Ser. A **271**, 105 (1963).
- ¹⁷According to M. Escorne and A. Mauger [Phys. Rev. B **25**, 4674 (1982)] $J_{\text{NNN}} \approx \frac{1}{8}J_{\text{NN}}$.
- ¹⁸In this analysis we take the interaction between nearest-neighbor spins to be $J\vec{S}_1 \cdot \vec{S}_2$ with $S = \frac{5}{2}$.